Available online at www.sciencedirect.com
SCIENCE DIRECT®
ELSEVIER
Chaos, Solitons and Fractals 23 (2005) 207–220
CHAOS SOLITONS & FRACTALS
www.elsevier.com/locate/chaos

On limit cycle approximations in the van der Pol oscillator

Mirta S. Padín [a,*], Federico I. Robbio [b,1], Jorge L. Moiola [b], Guanrong Chen [c]

[a] *Unidad Académica Río Gallegos, Universidad Nacional de la Patagonia Austral, Z9400JZV Río Gallegos, Argentina*
[b] *CONICET and Depto. de Ingeniería Eléctrica y de Computadoras, Universidad Nacional del Sur, Av. Alem 1253, B8000CPB, Bahía Blanca, Argentina*
[c] *Department of Electronic Engineering, City University of Hong Kong, 83 Tat Chee Avenue, Kowloon, Hong Kong, PR China*

Accepted 5 April 2004

Abstract

This paper applies bifurcation analysis to the well-known van der Pol oscillator to obtain approximations of its periodic solutions in the nearly sinusoidal regime. A frequency domain method based on harmonic balance approximations is used for small values of the bifurcation parameter. Moreover, a comparison with some other frequency domain approaches is also given. Finally, a total harmonic distortion is computed using the information provided by the frequency domain approach.

1. Introduction

Bifurcation analysis is an important mathematical tool for computing approximations of periodic solutions in some classical electronic oscillators (van der Pol, Colpitts, and so on), particularly in the nearly sinusoidal regime. Several methods have been proposed in the past [8,11,12], not only to analyze the dynamic behaviors of these oscillators but also to provide reliable tools for assisting circuit design in order to minimize harmonic distortions. Notably, many of them have been developed in the time domain using the perturbation theory [3]. Some others, like the one presented here, are performed in the frequency domain, i.e., utilizing the Laplace transforms, harmonic balance approximations, and Nyquist diagrams [1,13].

In most sinusoidal oscillator configurations, oscillation occurs when an equilibrium point loses its stability and a limit cycle emerges, that is, under the mechanism of the Hopf bifurcation theorem which relates the emergence of a periodic solution after a change of stability of the equilibrium point through a suitable variation of a key system parameter [14].

In general, calculating the steady-state waveform of nearly sinusoidal nonlinear oscillators requires the knowledge of its amplitude and frequency. Two principal items should be analyzed: how to establish the conditions to be met by the circuit to ensure the existence of a stable periodic oscillation and how to obtain an analytical representation of the oscillation for predicting the parameters of interest, particularly its amplitude and frequency.

The graphical Hopf bifurcation theorem (GHBT) in the frequency domain takes advantage of local predictions obtained by applying different higher-order harmonic balance approximations [13,16]. This method is useful

* Corresponding author.
E-mail addresses: mpadin@uarg.unpa.edu.ar (M.S. Padín), frobbio@criba.edu.ar (F.I. Robbio), jmoiola@criba.edu.ar (J.L. Moiola), eegchen@cityu.edu.hk (G. Chen).
[1] Fax: +54-291-4595154.

0960-0779/$ - see front matter © 2004 Elsevier Ltd. All rights reserved.
doi:10.1016/j.chaos.2004.04.018

for characterizing oscillations in nonlinear feedback systems with smooth nonlinearities, when a parameter is varied in the mathematical model. The main advantages of this approach rely on the graphical capabilities, similarly to the describing function method, and the explicit expressions of the harmonics. On the other hand, its main disadvantage relates to the crafty method required to obtain an adequate system realization such that the computation effort is minimized. Furthermore, if the system is highly nonlinear or the bifurcation parameter is far away from the critical value, higher-order bifurcation formulas are needed to obtain a better prediction or to study more complex phenomena like period-doubling bifurcation, quasi-periodic motion, bifurcation of cycles, and so on [5,6,18].

Other approaches in the frequency domain have helped in finding a first-order approximation of the periodic solution of interest and the bifurcation of the cycles using the describing function method [4]. With those methods it is possible to compute approximate values of the first period-doubling bifurcation, and some initial conditions of various complex dynamics, etc. based on simple engineering arguments and tools [9,10]. In order to show some comparisons with the results provided by GHBT, the method developed by Buonomo and colleagues [7,8] will be used, because it shares a similar flavor of higher-order expansions.

The rest of this paper is organized as follows. In Section 2, the GHBT in the frequency domain is briefly reviewed. In Section 3, general discussion on harmonic distortions is given. In Section 4, the main results obtained for the van der Pol circuit are presented, for both the GHBT and Buonomo's methods. Finally, some concluding remarks are given in the last section.

2. The frequency domain approach

Consider the following parametric autonomous system:

$$\begin{aligned} \dot{x} &= Ax + BDy + B[g(y;\varepsilon) - Dy], \\ y &= Cx, \end{aligned}$$

where $x \in R^n$, $y \in R^m$, A, B, C and D are $n \times n$, $n \times l$, $m \times n$ and $l \times m$ matrices, $\varepsilon \in R$ is the bifurcation (control) parameter, y is the output and $g : R^m \to R^l$ is a C^{2q+1}-function, where $2q$ is the order of smoothness and, equivalently, of the $2q$-order of harmonic balance approximation.

Following the results of [14], the system can be separated into two parts, the linear transfer matrix $G(s;\varepsilon)$ and the nonlinear feedback part $f(e;\varepsilon)$, as follows:

$$\begin{aligned} G(s;\varepsilon) &= C[sI - (A + BDC)]^{-1}B, \\ u &= f(e;\varepsilon) := g(y;\varepsilon) - Dy, \end{aligned}$$

where $y = -e$. It can be verified that the equilibrium points $\hat{e}$ are the solutions of the following equation:

$$G(0;\varepsilon)f(e;\varepsilon) = -e.$$

After solving for $\hat{e}$, the Jacobian matrix J of the nonlinear function $f(e;\varepsilon)$ is obtained as $J = (D_e f)_{e=\hat{e}}$, which is the linearization of the feedback function about the equilibrium point $\hat{e}$.

The eigenvalues of the open-loop matrix $G(s;\varepsilon)J$ are given by

$$h(\lambda, s;\varepsilon) = \det[\lambda I - GJ] = \lambda^p + a_{p-1}(s;\varepsilon)\lambda^{p-1} + \cdots + a_0(s;\varepsilon), \tag{1}$$

where $p = \min[\mathrm{rank}G, \mathrm{rank}J]$ and $a_i(\cdot)$ are rational functions of s.

Assuming a single root of $h(\cdot)$ at $\lambda = -1$ and replacing $s = \mathrm{i}\omega$ in (1), one has

$$h(-1, \mathrm{i}\omega;\varepsilon) = (-1)^p + \sum_{k=0}^{p-1}(-1)^k a_k(\mathrm{i}\omega;\varepsilon) = 0. \tag{2}$$

The pair $(\omega_0, \varepsilon_0)$ satisfying (2) corresponds to a necessary condition for obtaining a bifurcation point. If $\omega_0 = 0$, the bifurcation condition is called *static* and it is related to the multiplicity of the equilibrium point $\hat{e}$. On the other hand, if $\omega_0 \neq 0$, the bifurcation condition is known as *dynamic* or *Hopf* and it is related to the appearance of a branch of periodic solutions (if some other conditions are also satisfied).

Separating (2) in real (Re) and imaginary (Im) parts yields

$$\mathrm{Re}[h(-1,\mathrm{i}\omega;\varepsilon)] = F_1(\omega,\varepsilon) = (-1)^p + \sum_{k=0}^{p-1}(-1)^k\mathrm{Re}[a_k(\mathrm{i}\omega;\varepsilon)] = 0,$$

$$\mathrm{Im}[h(-1,\mathrm{i}\omega;\varepsilon)] = F_2(\omega,\varepsilon) = \sum_{k=1}^{p-1}(-1)^k\mathrm{Im}[a_k(\mathrm{i}\omega;\varepsilon)] = 0.$$

Then, the three basic statements of the Hopf bifurcation theorem in the frequency domain setting are given as follows:

(H1) There is only one eigenvalue $\hat{\lambda}$ of $h(\lambda,\mathrm{i}\omega;\varepsilon) = 0$ passing through the critical point $(-1+i0)$ when ω varies in $[0,\infty)$, in such a way that there is a change in the stability of the equilibrium solution. Moreover, there is only one frequency $\omega_0 \neq 0$ satisfying Eq. (2) for a given $\varepsilon = \varepsilon_0$ i.e., a resonance condition is avoided, and $\partial F_1/\partial\omega(\omega_0,\varepsilon_0)$, $\partial F_2/\partial\omega(\omega_0,\varepsilon_0)$ are not simultaneously zero. This condition excludes the situation where the locus of the eigenvalue $\hat{\lambda}$ has a loop and passes again the critical point with another frequency. The failure of this condition can give a double-zero root (Bogdanov–Takens bifurcation), one single-zero root plus a Hopf bifurcation condition (Gavrilov–Guckenheimer bifurcation), two pairs of imaginary roots (double Hopf bifurcation), and so on.

(H2) The following determinant is nonzero:

$$M = \begin{bmatrix} \dfrac{\partial F_1}{\partial\varepsilon} & \dfrac{\partial F_2}{\partial\varepsilon} \\ \dfrac{\partial F_1}{\partial\omega} & \dfrac{\partial F_2}{\partial\omega} \end{bmatrix}_{(\omega_0,\varepsilon_0)} \neq 0.$$

This condition guarantees the crossing of the bifurcating eigenvalue through the critical point $(-1+i0)$ with a nonzero speed of change.

(H3) The expression

$$\sigma_1 = -\mathrm{Re}\left\{\frac{u^{\mathrm{T}}G(\mathrm{i}\omega_0;\varepsilon)p_1(\omega_0;\varepsilon)}{u^{\mathrm{T}}G'(\mathrm{i}\omega_0;\varepsilon)Jv}\right\}, \tag{3}$$

called the *curvature coefficient*, does not change its sign when ε varies near ε_0. In the above formula, u^{T} and $v = [v_1\ \ v_2\ \ \cdots\ \ v_p\ \ \cdots\ \ v_n]^{\mathrm{T}}$ are the left and right eigenvectors of the open-loop transfer matrix $[G(\mathrm{i}\omega;\varepsilon)J(\varepsilon)]$ associated with $\hat{\lambda}$, $G'(\mathrm{i}\omega_0;\varepsilon) = \mathrm{d}G/\mathrm{d}s_{s=\mathrm{i}\omega_0}$ and p_1 is given by

$$p_1(\omega,\varepsilon) = QV_{02} + \frac{1}{2}\overline{Q}V_{22} + \frac{1}{8}L\overline{v}, \tag{4}$$

where

$$V_{02} = -\frac{1}{4}H(0;\varepsilon)Q\overline{v},$$
$$V_{22} = -\frac{1}{4}H(\mathrm{i}2\omega;\varepsilon)Qv,$$

and "$\overline{\ \ }$" denotes the complex conjugate, $H(s;\varepsilon) := [G(s;\varepsilon)J + I]^{-1}G(s;\varepsilon)$ is the closed-loop transfer matrix; the $l \times m$ matrices Q and L are

$$Q = [Q_{jk}] = \left[\sum_{p=1}^{m}\frac{\partial^2 f_j}{\partial e_p\partial e_k}\bigg|_{\hat{e}} v_p\right],$$

and

$$L = [L_{jk}] = \left[\sum_{p=1}^{m}\sum_{q=1}^{m}\frac{\partial^3 f_j}{\partial e_p\partial e_q\partial e_k}\bigg|_{\hat{e}} v_p v_q\right],$$

where $j = 1,2,\ldots,l$, $k = 1,2,\ldots,m$. Eq. (3) is the so-called stability index (or, Lyapunov coefficient, focal value) which indicates the stability of the emerging periodic solution at the *criticality*, i.e., it determines if the Hopf bifurcation is supercritical or subcritical.

In order to obtain approximations of the periodic solutions in the neighborhood of the criticality, it is necessary to evaluate Eq. (4) and the eigenvectors at a frequency $\omega = \omega_R$, where ω_R is obtained by solving $\mathrm{Im}\{\hat{\lambda}(\mathrm{i}\omega_R)\} = 0$, and $\mathrm{Re}\{\hat{\lambda}(\mathrm{i}\omega_R)\} = 0$ is the closest value to the critical point $(-1 + i0)$.

The amplitude $\hat{\theta}$ and a better estimation of the frequency $\hat{\omega}$ of the oscillations are obtained by solving the following expression:

$$\hat{\lambda}(\mathrm{i}\hat{\omega}) = -1 + \xi_1(\omega_R)\hat{\theta}^2, \tag{5}$$

where $\xi_1(\omega_R) = -\frac{u^{\mathrm{T}} G(\mathrm{i}\omega_R) p_1(\omega_R;\varepsilon)}{u^{\mathrm{T}} v}$ for the second-order harmonic balance, or

$$\hat{\lambda}(\mathrm{i}\hat{\omega}) = -1 + \sum_{k=1}^{2q} \xi_k(\mathrm{i}\hat{\omega})\hat{\theta}^{2k}, \tag{6}$$

for a $2q$th-order harmonic balance, where ξ_k are given in [13,16].

Finally, the approximation formulas for the second-order harmonic balance are given by

$$e(t) = \hat{e} + \mathrm{Re}\left\{ \sum_{k=0}^{2} E^k \exp(\mathrm{i}k\hat{\omega}t) \right\}, \tag{7}$$

where $E^0 = \theta^2 V_{02}$, $E^1 = \theta v$ and $E^2 = \theta^2 V_{22}$, while the equivalent generalization for the $2q$th-order harmonic balance is expressed as

$$e(t) = \hat{e} + \mathrm{Re}\left\{ \sum_{k=0}^{2q} E^k \exp(\mathrm{i}k\hat{\omega}t) \right\}, \tag{8}$$

where $E^0 = \theta^2 V_{02} + \theta^4 V_{04} + \theta^6 V_{06} + \cdots + \theta^{2q} V_{0,2q}$, $E^1 = \theta v + \theta^3 V_{13} + \theta^5 V_{15} + \cdots + \theta^{2q+1} V_{1,2q+1}$, $E^2 = \theta^2 V_{22} + \theta^4 V_{24} + \theta^6 V_{26} + \cdots + \theta^{2q} V_{2,2q}$ and $E^k = \theta^k V_{kk} + \theta^{k+2} V_{k,k+2} + \cdots$ are given explicitly in [13,16] up to the order $2q = 8$. This method will be applied to the van der Pol circuit in Section 4.

3. Harmonic distortion

Harmonic distortion is an important measure of the quality of the waveform of an oscillator [15] and it allows to compare the amplitude of the fundamental frequency with its harmonics.

According to the formulas given in the previous section, the amplitudes of higher-order harmonics depend on the parameter ε. The signal $e_{\mathrm{T}}(t)$ is a sum of its harmonic components, assuming that there is no DC component on it:

$$e_{\mathrm{T}}(t) = e_{\mathrm{f}}(t) + \sum_{i \neq 1} e_{\mathrm{h}_i}(t),$$

where e_{f} is the fundamental component of the signal to be examined and e_{h_i} is the component at the i harmonic.

The root-mean-square (rms) values are calculated using the well-known definition

$$E_{\mathrm{T}} = \left(\frac{1}{T} \int_0^{\mathrm{T}} e_{\mathrm{T}}^2(t)\,\mathrm{d}t \right)^{\frac{1}{2}}, \quad \text{or} \quad E_{\mathrm{T}} = \left(E_{\mathrm{F}}^2 + \sum_{i \neq 1} E_{\mathrm{h}_i}^2 \right)^{\frac{1}{2}}.$$

The amount of distortion in the signal waveform is quantified by means of an index called *total harmonic distortion* (THD).

The distortion component of the signal is related directly with its harmonics:

$$e_{\mathrm{d}}(t) = e_{\mathrm{T}}(t) - e_{\mathrm{f}}(t),$$

and, in terms of rms values,

$$E_{\mathrm{d}} = (E_{\mathrm{T}}^2 - E_{\mathrm{F}}^2)^{\frac{1}{2}}.$$

The THD is then given by

$$\%\mathrm{THD} = 100 \frac{E_{\mathrm{d}}}{E_{\mathrm{f}}}.$$

4. The van der Pol circuit

4.1. The circuit model

The well-known van der Pol's equation is given by

$$\ddot{x} + \varepsilon(x^2 - 1)\dot{x} + x = 0, \tag{9}$$

which is a simple harmonic oscillator with a nonlinear damped term, $\varepsilon(x^2 - 1)\dot{x}$. This term acts as a positive damping for $|x| > 1$, producing a decay in large amplitude oscillations, while for $|x| < 1$ this damping is negative producing an increment in the response. The consequence is that the system builds in a self-sustained oscillation where the dissipated energy over a cycle is balanced with the acquired energy. This reasoning justifies roughly why the van der Pol equation has only one stable limit cycle for each $\varepsilon > 0$.

In terms of the first-order variable representation, Eq. (9) yields

$$\begin{aligned} \dot{x}_1 &= x_2, \\ \dot{x}_2 &= -x_1 - \varepsilon\left(x_1^2 - 1\right)x_2. \end{aligned} \tag{10}$$

The corresponding linearized system has pure imaginary eigenvalues when $\varepsilon = 0$, so it may seem that the bifurcation condition appears. However, for $0 < \varepsilon \ll 1$, the system has a stable limit cycle, and for $\varepsilon < 0$ an unstable limit cycle appears. This situation is directly related with the fact that $\varepsilon = 0$ is a degenerate bifurcation because the nonlinear terms disappear and the curvature coefficient given by Eq. (3) is equal to zero. As explained in [14], the van der Pol oscillator does not satisfy the Hopf bifurcation theorem because the emergence of the limit cycle is not born out of the equilibrium.

In order to apply the technique proposed in Section 2, a change of variables is needed to remove the degeneracy, in a way suggested by [19]:

$$u = \varepsilon^{\frac{1}{2}}x, \quad \varepsilon > 0. \tag{11}$$

Then, Eq. (9) changes to

$$\ddot{u} + u + u^2\dot{u} - \varepsilon\dot{u} = 0. \tag{12}$$

However, this change of variables modifies the nature of the periodic solution of the original Eq. (9) as it will be explained below. Analyzing the original van der Pol system (9), unstable limit cycles are obtained for $\varepsilon < 0$. However, considering the change of variables proposed in Eq. (11) the Hopf bifurcation emerging in Eq. (12) is supercritical: only stable limit cycles are detected for $\varepsilon > 0$ after a change of the stability of the equilibrium solution. Since one is interested in approximating stable periodic solutions for $\varepsilon > 0$, assume that Eq. (11) is a suitable transformation for this purpose.

Finally, Eq. (12) can be written as

$$\begin{aligned} \dot{u}_1 &= -u_2 + \varepsilon u_1 - \frac{1}{3}u_1^3 \\ \dot{u}_2 &= u_1, \end{aligned} \tag{13}$$

which is easily verified by taking time-derivative of the first equation, i.e., $\frac{\mathrm{d}\dot{u}_1}{\mathrm{d}t} = \ddot{u}_1 = -\dot{u}_2 + \varepsilon\dot{u}_1 - u_1^2\dot{u}_1$. Then, by using $\dot{u}_2 = u_1$ and assigning $u = u_1$, Eq. (12) follows. Eq. (13) is called the *modified* van der Pol circuit. It is important to note that the nonlinearity is now in one state variable and this simplifies the following calculations.

4.2. Main results

To apply the frequency domain method [14] to the modified van der Pol equation (13), the following realization is proposed:

$$A = \begin{pmatrix} -1 & -1 \\ 1 & 0 \end{pmatrix}; \quad B = \begin{pmatrix} 1 \\ 0 \end{pmatrix}; \quad C = [1 \quad 0]; \quad D = 0.$$

In this case, the nonlinear term is $g(u_1;\varepsilon) = (1+\varepsilon)u_1 - \frac{1}{3}u_1^3$, and the transfer function is

$$G(s) = C(sI - A)^{-1}B = \frac{s}{s^2 + s + 1},$$

where

$$y_1 = u_1 = -e_1; \quad f(e_1;\varepsilon) = -(1+\varepsilon)e_1 + \frac{1}{3}e_1^3, \quad G(0)f(e_1;\varepsilon) = 0 = -e_1.$$

The equilibrium point is $\hat{e}_1 = 0$, and the Jacobian is

$$J = -(1+\varepsilon) + \hat{e}_1^2|_{\hat{e}_1-0} = -(1+\varepsilon).$$

The eigenvalue $\hat{\lambda} = G(s)J|_{s=\mathrm{i}\omega}$ at the bifurcation condition is

$$\hat{\lambda} = -1 = \frac{-(1+\varepsilon)\mathrm{i}\omega}{(1-\omega^2)+\mathrm{i}\omega}.$$

Solving its real and imaginary parts, the frequency for ω_0 is $\omega_0 = \omega_{\mathrm{Hopf}} = 1$ for $\varepsilon = 0$. To obtain $\hat{\lambda}(\mathrm{i}\omega_R)$, where ω_R satisfies $\mathrm{Im}\{\hat{\lambda}(\mathrm{i}\omega_R)\} = 0$ the resulting frequency yields also $\omega_R = \omega_{\mathrm{Hopf}} = 1$.

The left and right eigenvectors are $u^{\mathrm{T}} = 1$, $v = V_{11} = 1$ since the system is SISO (single-input single-output). Following the procedure described in the previous section, one obtains $V_{02} = V_{22} = 0$, $p_1 = \frac{1}{4}$ and $\xi_1 = -\frac{1}{4}$. Then $\hat{\lambda}|_{\omega=\omega_R} \approx -(1+\varepsilon) = -1 - \frac{1}{4}\theta^2$ So, it is easy to obtain

$$\theta = 2\sqrt{\varepsilon}. \tag{14}$$

Finally, the response is expressed as

$$\begin{aligned} E^1 &= v\theta = 2\sqrt{\varepsilon}, \\ e_1(t) &= \mathrm{Re}\{2\sqrt{\varepsilon}(\cos t + \mathrm{i}\sin t)\} = 2\sqrt{\varepsilon}\cos t, \\ u_1(t) &= -e_1 = -2\sqrt{\varepsilon}\cos t. \end{aligned} \tag{15}$$

Returning to the original variable (applying the scale of Eq. (11)), it follows that

$$x_1(t) = -2\cos t. \tag{16}$$

In order to construct a more accurate approximation, by noticing that the system is SISO, it yields $V_{13} = V_{15} = \cdots = V_{1,2q+1} = 0$. Suppose, for simplicity, that the estimation of the frequency $\omega_R = 1$ is appropriate and there is no need of correction. Then, a fourth-order harmonic expansion (see the formulas in [13]) gives

$$V_{22} = V_{02} = V_{04} = V_{24} = V_{44} = 0$$

$$V_{33} = \frac{1}{4\sqrt{64+9\varepsilon^2}} \exp\left[\mathrm{i}\left(\Phi_{33} + \frac{\pi}{2}\right)\right], \quad E^3 = \theta^3 V_{33},$$

where $\phi_{33} = \arctan(\frac{-3\varepsilon}{8})$. The solution in terms of $e_1(t)$ can be expressed as

$$e_1(t,\varepsilon) = \mathrm{Re}\{E^1\exp(\mathrm{i}t) + E^3\exp(3\mathrm{i}t)\} = 2\sqrt{\varepsilon}\cos t + \frac{2\varepsilon\sqrt{\varepsilon}}{\sqrt{64+9\varepsilon^2}}\cos\left(3t + \Phi_{33} + \frac{\pi}{2}\right),$$

while the one in the original variable would be corrected in the following way:

$$x_1(t,\varepsilon) = -2\cos t - \frac{2\varepsilon}{\sqrt{64+9\varepsilon^2}}\cos\left(3t + \frac{\pi}{2} + \Phi_{33}\right) = -2\cos t + \frac{2\varepsilon}{\sqrt{64+9\varepsilon^2}}\sin(3t + \Phi_{33}). \tag{17}$$

Without making corrections in amplitude and frequency through Eq. (6), and to obtain quasi-analytical approximations, the expansion in six harmonics (see the formulas in [16]) is

$$V_{35} = \frac{-3}{8(64+9\varepsilon^2)}\exp[\mathrm{i}2\Phi_{33}],$$

$$V_{06} = V_{26} = 0, \quad V_{17} = 0,$$

$$V_{55} = \frac{-5}{16\sqrt{576+25\varepsilon^2}\sqrt{64+9\varepsilon^2}}\exp[\mathrm{i}(\Phi_{33} + \Phi_{55})],$$

where $\Phi_{55} = \arctan(\frac{-5\varepsilon}{24})$. This means that the amplitude and frequency are fixed by the second-order harmonic balance at $\theta = 2\sqrt{\varepsilon}$ and $\omega_R = 1$, respectively. The computation is carried out by using Algorithm 1 shown in Appendix A.

It is important to highlight the validity of the approximation. As the series is expanded in terms of the parameter θ, it should require $\theta < 1$ so as to guarantee the convergence, at least conservatively. Notice that the higher-order terms $V_{33}, V_{35}, V_{55}, \ldots$, and therefore ξ_1, ξ_2 and ξ_3, are decreasing in absolute value due to the property of low-pass filter of the transfer function $G(s)$. So, the contribution of the higher-order harmonics is certainly attenuated for small values of ε. Thus, it can be easily deduced that if $\theta < 1$ then $\varepsilon < \frac{1}{4}$. Thus, a conservative estimate of the limit of the convergence, ε should be slightly greater than $\frac{1}{4}$ if ξ_1, ξ_2, ξ_3 satisfy the decreasing modulus property, which is a standard feature of physical systems.

Relying on the same simplifications as before (i.e., $\theta = 2\sqrt{\varepsilon}$ and $\omega_R = 1$), the approximate solution using sixth-order harmonic balance can be written as

$$x_1^{\mathrm{MC}}(t,\varepsilon) = -2\cos t + \frac{2\varepsilon}{\sqrt{64+9\varepsilon^2}}\sin(3t+\Phi_{33}) + \frac{12\varepsilon^2}{64+9\varepsilon^2}\cos(3t+2\Phi_{33}) + \frac{10\varepsilon^2}{\sqrt{64+9\varepsilon^2}\sqrt{576+25\varepsilon^2}}\cos(5t+\Phi_{33}+\Phi_{55}), \tag{18}$$

where the superscript MC means the approximate solution obtained using Mees–Chua's method without updating the amplitude $\hat{\theta}$ and frequency $\hat{\omega}$ through Eq. (6). Notice that the associate coefficients in ε in Eq. (18) can be expanded in Taylor series around $\varepsilon = 0$, as follows:

$$\frac{2\varepsilon}{\sqrt{64+9\varepsilon^2}} = \frac{1}{4}\varepsilon - \frac{9}{512}\varepsilon^3 + \frac{243}{131072}\varepsilon^5 + \cdots$$

$$\frac{12\varepsilon^2}{(64+9\varepsilon^2)} = \frac{3}{16}\varepsilon^2 - \frac{27}{1024}\varepsilon^4 + \frac{243}{65536}\varepsilon^6 + \cdots$$

$$\frac{10\varepsilon^2}{\sqrt{64+9\varepsilon^2}\sqrt{576+25\varepsilon^2}} = \frac{5}{96}\varepsilon^2 - \frac{530}{110592}\varepsilon^4 + \frac{5335}{10616832}\varepsilon^6 + \cdots$$

Thus, Eq. (18) can be rewritten in terms of the expansion in ε in order to compare with other formulations:

$$x_1^{\mathrm{MC}}(t,\varepsilon) = -2\cos t + \left(\frac{1}{4}\varepsilon - \frac{9}{512}\varepsilon^3 + \frac{243}{131072}\varepsilon^5 + \cdots\right)\sin(3t+\Phi_{33}) + \left(\frac{3}{16}\varepsilon^2 - \frac{27}{1024}\varepsilon^4 + \frac{243}{65536}\varepsilon^6 + \cdots\right) \times \cos(3t+2\Phi_{33}) + \left(\frac{5}{96}\varepsilon^2 - \frac{530}{110592}\varepsilon^4 + \frac{5335}{10616832}\varepsilon^6 + \cdots\right)\cos(5t+\Phi_{33}+\Phi_{55}). \tag{19}$$

Notice that Eqs. (10) and (13) have the symmetry $x_1 \to -x_1, x_2 \to -x_2$ and $u_1 \to -u_1, u_2 \to -u_2$, respectively. So, multiplying Eq. (19) by -1 also gives a solution. Thus, an equivalent valid solution for the sixth-order harmonic balance approximation with an expansion in ε is

$$-x_1^{\mathrm{MC}}(t) = x_{1\mathrm{equiv}}^{\mathrm{MC}}(t) = 2\cos t + \left(-\frac{1}{4}\varepsilon + \frac{9}{512}\varepsilon^3 - \frac{243}{131072}\varepsilon^5 + \cdots\right)\sin(3t+\Phi_{33}) - \left(\frac{3}{16}\varepsilon^2 - \frac{27}{1024}\varepsilon^4 + \frac{243}{65536}\varepsilon^6 + \cdots\right)\cos(3t+2\Phi_{33}) - \left(\frac{5}{96}\varepsilon^2 - \frac{530}{110592}\varepsilon^4 + \frac{5335}{10616832}\varepsilon^6 + \cdots\right)\cos(5t+\Phi_{33}+\Phi_{55}). \tag{20}$$

This explicit non-updated solution can be compared to the expansion obtained by [8] for second-order in ε:

$$x_1^{B,2}(t,\varepsilon) = 2\cos(\omega t) - \frac{\varepsilon}{4}\sin(3\omega t) - \varepsilon^2\left(\frac{3}{32}\cos(3\omega t) + \frac{5}{96}\cos(5\omega t)\right), \tag{21}$$

where

$$\omega = 1 - \frac{1}{16}\varepsilon^2 + O(\varepsilon^4),$$

or by [7] up to the fourth-order approximation in ε, as follows

$$x_1^{B,4}(t,\varepsilon) = \left(2 + \frac{1}{64}\varepsilon^2 - \frac{23}{49152}\varepsilon^4\right)\cos(\omega t) + \left(-\frac{1}{4}\varepsilon - \frac{15}{512}\varepsilon^3 + \cdots\right)\sin(3\omega t) + \left(-\frac{3}{32}\varepsilon^2 + \frac{101}{12288}\varepsilon^4 + \cdots\right) \times \cos(3\omega t) - \frac{85}{2304}\varepsilon^3\sin(5\omega t) + \left(-\frac{5}{96}\varepsilon^2 + \frac{1865}{110592}\varepsilon^4 + \cdots\right)\cos(5\omega t) - \frac{7}{576}\varepsilon^3\sin(7\omega t) + \frac{1379}{110592}\varepsilon^4\cos(7\omega t) + \frac{61}{20480}\varepsilon^4\cos(9\omega t) + O(\varepsilon^5), \tag{22}$$

and

$$\omega = 1 - \frac{1}{16}\varepsilon^2 + \frac{17}{3072}\varepsilon^4 + O(\varepsilon^6). \tag{23}$$

As can be easily seen from Eqs. (20) and (22), there is no improvement in Mees and Chua's method in correcting the approximation of the amplitude of the first harmonic in terms of ε. So, it is important to use the updated algorithm on amplitude $\hat{\theta}_k$ and frequency $\hat{\omega}_k$, $k = 2, 3, 4$, provided by the following expressions:

$$\hat{\lambda}(\mathrm{i}\omega_2) = \frac{-(1+\varepsilon)\mathrm{i}\omega_2}{(1-\omega_2^2)+\mathrm{i}\omega_2} = -1 + \xi_1(\omega_2)\theta^2 + \xi_2(\omega_2)\theta^4, \tag{24}$$

$$\hat{\lambda}(\mathrm{i}\omega_3) = -1 + \xi_1(\omega_3)\theta^2 + \xi_2(\omega_3)\theta^4 + \xi_3(\omega_3)\theta^6, \tag{25}$$

and

$$\hat{\lambda}(\mathrm{i}\omega_4) = -1 + \xi_1(\omega_4)\theta^2 + \xi_2(\omega_4)\theta^4 + \xi_3(\omega_4)\theta^6 + \xi_4(\omega_4)\theta^8, \tag{26}$$

where ξ_2, ξ_3 and ξ_4 are given in Appendix A, and it is called the *iterative graphical method* (IGM). These expressions can be solved graphically in a manner reminiscent to the describing function method in the following way: the solution set $(\hat{\omega}_2, \hat{\theta}_2)$ satisfies $\hat{\lambda}(\mathrm{i}\omega_{2,k}) = -1 + \xi_1(\omega_{2,k-1})\hat{\theta}^2 + \xi_2(\omega_{2,k-1})\hat{\theta}^4$ when $\omega_{2,k} \cong \omega_{2,k-1}$. Analogous solutions correspond to Eqs. (25) and (26).

This algorithm has been suggested by [14], used profusely by [16], and recently by [18], for detecting several bifurcations of the cycles close to Hopf bifurcations.

Figs. 1 and 2 show the output waveform obtained by numerical simulations (NS), Buonomo's method (BM), a sixth-order harmonic balance by using GHBT (Eq. (19)) and an eighth-order harmonic balance IGM for $\varepsilon = 0.5$ and $\varepsilon = 0.8$, respectively. Since the GHBT does not update frequency and amplitude, their results are clearly distinguishable from the rest.

A measure for comparing the oscillatory predictions by varying the parameter ε is constructed using the maximum amplitude of the oscillation versus the bifurcation parameter. This is the bifurcation diagrams for the BM, GHBT, IGM and NS shown in Fig. 3. In this figure, both analytical approximations given by Eqs. (18) and (22), i.e., GHBT and BM, behave quite similarly. Moreover, the updated algorithm (IGM) has very good predictions of the amplitude up to $\varepsilon = 0.7$ The conservative prediction of $\varepsilon \approx 0.25$ by the frequency domain method (GHBT and IGM) can be extended

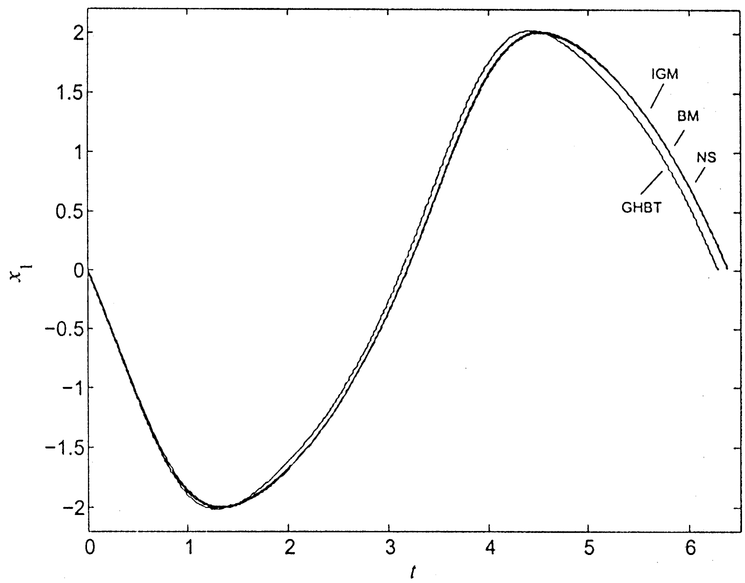

Fig. 1. Output waveform obtained by Buonomo's method (BM), the non-updated algorithm (GHBT), the iterative graphical method (IGM) and numerical simulations (NS), for $\varepsilon = 0.5$.

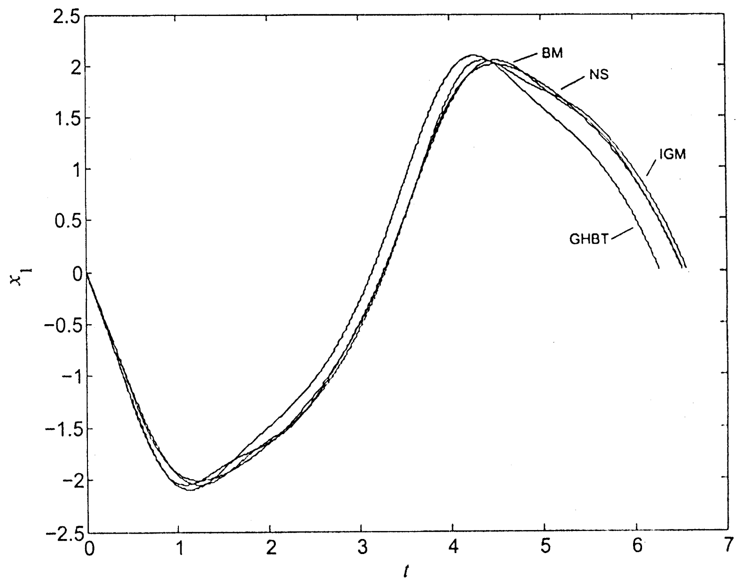

Fig. 2. Output waveform obtained by Buonomo's method (BM), the non-updated algorithm (GHBT), the iterative graphical method (IGM) and numerical simulations (NS), for $\varepsilon = 0.8$.

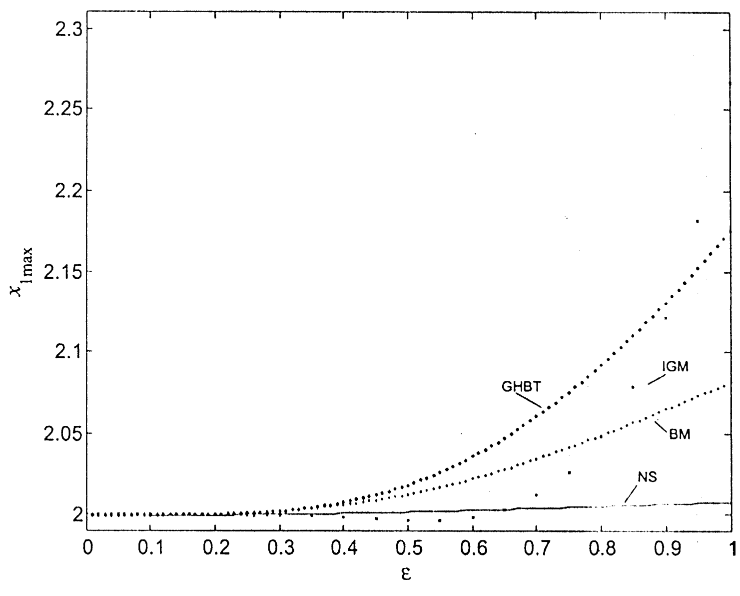

Fig. 3. Maximum amplitude of the oscillation for the van der Pol circuit using Buonomo's method (+), GHBT (◊), IGM (×) and numerical simulations NS (−−).

slightly far away from $\varepsilon \approx 0.50$. In [7], it is shown that the validity of the convergence of the series goes up to $\varepsilon < 1.89$. It is important to emphasize here that the expansion in ε is truncated to the fourth-order term, as Eq. (22) shows. However, other indexes to measure the accuracy of the approximations can be used in order to make better conclusions.

Another interesting feature with the IGM is the correction of the frequency in terms of the parameter ε. According to [2], who obtained an expansion up to the order $O(\varepsilon^{24})$ in rational arithmetic, the expansion of the frequency ω in terms of ε (for simplicity up to the order $O(\varepsilon^{14})$), is given by

$$\omega = 1 - \frac{1}{16}\varepsilon^2 + \frac{17}{3072}\varepsilon^4 + \frac{35}{884736}\varepsilon^6 - \frac{678899}{5096079360}\varepsilon^4 + \frac{28160413}{2293235712000}\varepsilon^{10} + \frac{16729607288111}{3698530556313600000}\varepsilon^{12} + O(\varepsilon^{14}). \tag{27}$$

A comparison of the frequency variation in terms of ε with the IGM and Eq. (27) is shown in Fig. 4. This last curve is denoted as AG in the graph, and it is computed up to the order $O(\varepsilon^{24})$. The IGM gives a pretty good estimate of the frequency variation, considering the non-updated case which is fixed to $\omega = 1$.

Another measure of the approximations consists in plotting the departure from +1.00000 of the trivial Floquet multiplier of the linearized variational equation around the periodic solution. This trivial multiplier computed using

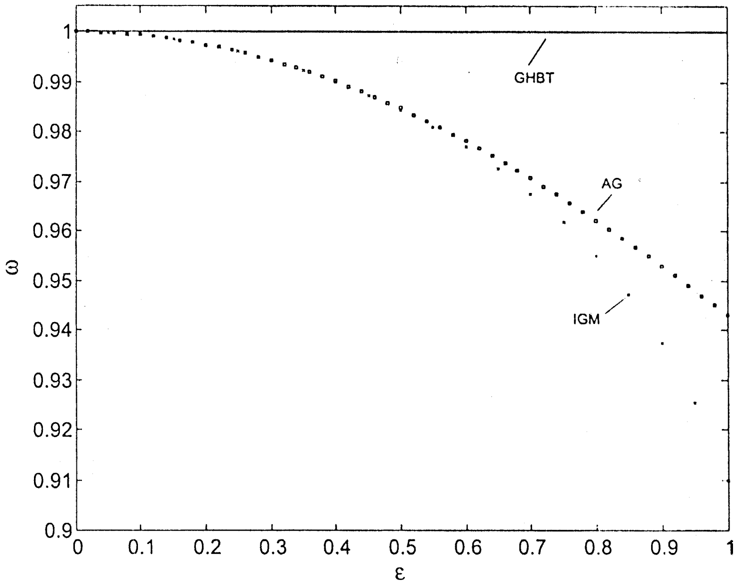

Fig. 4. Comparison of the variation in frequency ω obtained with the IGM ($\times$) and the expansion given by [2] ($\square$). The GHBT algorithm does not update the frequency ($\omega = 1$).

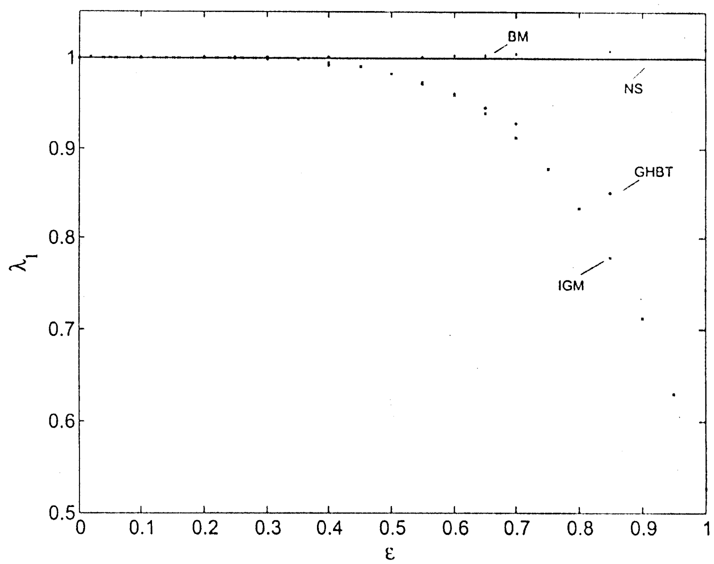

Fig. 5. Plot of the trivial Floquet multiplier for BM (+), GHBT ($\diamondsuit$), IGM ($\times$) and numerical simulations (——).

Table 1
%Total Harmonics Distortion versus ε

ε	%THD for BM	%THD for GHBT	%THD for QFM
0.01	0.125032	0.125006	0.124999
0.03	0.375156	0.375159	0.37498
0.05	0.625461	0.625734	0.624908
0.10	1.25281	1.25585	1.24927
0.124	1.55515	1.56112	1.54861
0.20	2.5206	2.54605	2.49422
0.30	3.82791	3.90143	3.73088
0.40	5.1584	5.34653	4.95598
0.50	6.55454	6.89808	6.1671
0.60	8.01746	8.56473	7.36284
0.70	9.55693	10.3477	8.54273
0.80	11.1814	12.2419	9.707
0.90	12.8983	14.2377	10.8562
1.00	14.7145	16.3217	11.9907

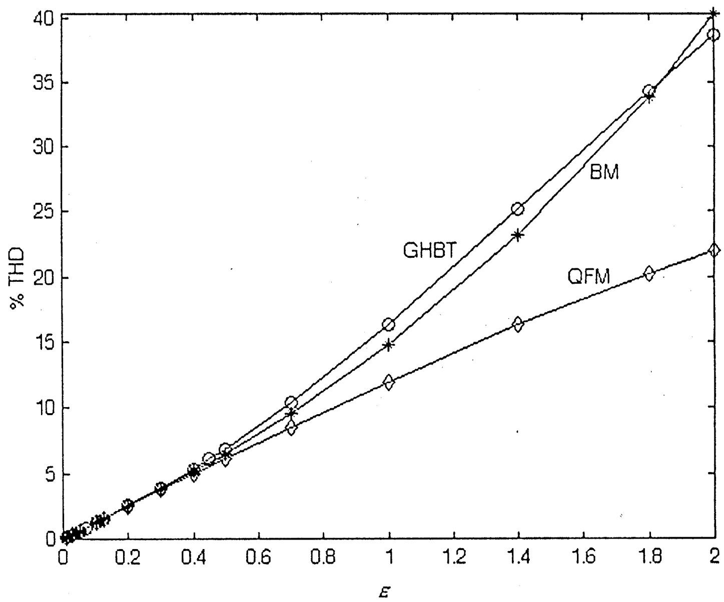

Fig. 6. Comparison of total harmonic distortion (%THD) using BM, GHBT and QFM.

Buonomo's method gives the best performance (more accurate approximation) as can be seen in Fig. 5. However, the non-updated algorithm (GHBT) as well as the IGM give good results even for $\varepsilon \approx 0.4 - 0.5$.

Both Buonomo and GHBT methods give the results presented in the two first columns of Table 1. These are plotted in Fig. 6 in terms of the total harmonic distortion (THD) versus the bifurcation parameter ε. Other approximations of the harmonic amplitudes have been presented by [17], referred as QFM in Fig. 6 and in the last column of Table 1. The total harmonic distortion is in accordance up to $\varepsilon \approx 0.8$ as compared to the BM and GHBT results. For $\varepsilon > 0.8$, the approximation provided by QFM gives less total harmonic distortion than that by BM and GHBT.

5. Conclusions

Some comparisons in approximating periodic solutions with two different higher-order harmonic balance methods have been shown on the van der Pol oscillator. The GHBT provides quite good results as compared to the IGM, taking into account that there is no need to implement an additional computational algorithm, i.e., their formulas are explicit.

This observation is also reinforced by adding other measures of accuracy as the departure from the key point +1.00000 of the trivial Floquet multiplier, the temporal waveform, the harmonic distortion, etc. On the other hand, the IGM gives a proper correction to the frequency in the same direction as do by other classical methods. For BM and GHBT, a computation of total harmonic distortion and the departure from +1.00000 of the trivial Floquet multiplier are calculated and depicted versus the main bifurcation parameter. Here, a third approximation is added (QFM) for the study of distortion. All methods seem reliable in the study of the distortion of higher-harmonics in the region of their respective convergence of series expansion.

Acknowledgements

F.I.R. and J.L.M. acknowledge the financial support of ANPCyT through grant PICT-2002-11-12524, CONICET and the SECyT of the UNS. J.L.M. and G.C. acknowledge the financial support of the Hong Kong Research Grants Council through CERG Grant 1115/03E.

Appendix A

1. The following two algorithms have the following common settings:

$$D_2 = \left.\frac{\partial^2 f}{\partial e_1^2}\right|_{e_1=0} = 0, \qquad D_3 = \left.\frac{\partial^3 f}{\partial e_1^3}\right|_{e_1=0} = 2, \qquad D_k = \left.\frac{\partial^k f}{\partial e_1^k}\right|_{e_1=0} = 0, \quad k > 3 \text{ and}$$

$$V_{0,2q} = V_{2,2q} = 0, \quad q = 1, 2, 3 \text{ and } 4,$$

$$V_{4,4+2q_1} = 0, \quad q_1 = 0, 1 \text{ and } 2,$$

$$V_{6,6+2q_2} = 0, \quad q_2 = 0 \text{ and } 1,$$

$$V_{13} = \ldots = V_{1,2q+1} = 0, \quad q = 1, 2, 3 \text{ and } 4.$$

Moreover, $E^1 = \theta$, $E^3 = \theta^3 V_{33} + \theta^5 V_{35} + \theta^7 V_{37}$, $E^5 = \theta^5 V_{55} + \theta^7 V_{57}$ and $E^7 = \theta^7 V_{77}$ and the periodic solution is given by $e_1(t) = \hat{e}_1 + \mathrm{Re}\{\sum_{k-0}^{3} E^{2k+1} \exp[\mathrm{i}(2k+1)\hat{\omega}t]\}$.

2. *Algorithm 1:* Computation of the complex numbers for the van der Pol oscillator without update:

$$v = V_{11} = 1, \quad \omega = 1, \quad \theta = 2\sqrt{\varepsilon}$$

$$V_{33} = \frac{1}{4\sqrt{64 + 9\varepsilon^2}} \exp\left[\mathrm{i}\left(\Phi_{33} + \frac{\pi}{2}\right)\right], \quad \Phi_{33} = \arctan\left(\frac{-3\varepsilon}{8}\right),$$

$$V_{35} = \frac{-3}{8(64 + 9\varepsilon^2)} \exp[\mathrm{i}2\Phi_{33}],$$

$$V_{55} = \frac{-5}{16\sqrt{576 + 25\varepsilon^2}\sqrt{64 + 9\varepsilon^2}} \exp[\mathrm{i}(\Phi_{33} + \Phi_{55})], \quad \Phi_{55} = \arctan\left(\frac{-5\varepsilon}{24}\right).$$

3. *Algorithm IGM:* Computation of the complex numbers for the van der Pol oscillator with update:

$$v = V_{11} = 1,$$

$$H(\mathrm{i}k\omega) = \frac{k\mathrm{i}}{1 - k^2\omega^2 - k\varepsilon\mathrm{i}}, k = 3, 5 \text{ and } 7,$$

$$\xi_1 = -\frac{1}{8} G(\mathrm{i}\omega) D_3.$$

Update $\hat{\omega}_1$ and $\hat{\theta}_1$ by solving $\hat{\lambda}(\mathrm{i}\hat{\omega}_1) = -1 + \xi_1(\omega_R)\hat{\theta}_1^2$, and re-calculate ξ_1 at $\hat{\omega}_1$. Compute

$$V_{33} = -\frac{1}{24} H(\mathrm{i}3\hat{\omega}_1) D_3,$$

$$\xi_2 = -\frac{1}{8} G(\mathrm{i}\hat{\omega}_1) D_3 V_{33}.$$

Update $\hat{\omega}_2$ and $\hat{\theta}_2$ by solving $\hat{\lambda}(\mathrm{i}\hat{\omega}) = -1 + \xi_1(\omega)\hat{\theta}^2 + \xi_2(\omega)\hat{\theta}^4$, and re-calculate ξ_1, ξ_2, and V_{33} at $\hat{\omega}_2$.
Compute

$$V_{35} = -\frac{1}{4}H(\mathrm{i}3\hat{\omega}_2)D_3V_{33},$$

$$V_{55} = -\frac{1}{8}H(\mathrm{i}5\hat{\omega}_2)D_3V_{33},$$

$$\xi_3 = -\frac{1}{8}G(\mathrm{i}\hat{\omega}_2)D_3\{V_{35} + 2V_{33}\overline{V}_{33}\}.$$

Update $\hat{\omega}_3$ and $\hat{\theta}_3$ by solving $\hat{\lambda}(\mathrm{i}\omega) = -1 + \xi_1(\omega)\hat{\theta}^2 + \xi_2(\omega)\hat{\theta}^4 + \xi_3(\omega)\hat{\theta}^6$, and re-calculate $\xi_1, \xi_2, \xi_3, V_{33}, V_{35}, V_{55}$ at $\hat{\omega}_3$. Compute

$$V_{37} = -H(\mathrm{i}3\hat{\omega}_3)D_3\left\{\frac{1}{4}V_{35} + \frac{1}{8}V_{55}\right\},$$

$$V_{57} = -H(\mathrm{i}5\hat{\omega}_3)D_3\left\{\frac{1}{8}V_{35} + \frac{1}{4}V_{55} + \frac{1}{8}V_{33}V_{33}\right\},$$

$$V_{77} = -H(\mathrm{i}7\hat{\omega}_3)D_3\left\{\frac{1}{8}V_{55} + \frac{1}{8}V_{33}V_{33}\right\},$$

$$\xi_4 = -\frac{1}{8}G(\mathrm{i}\hat{\omega}_3)D_3\{V_{37} + 2V_{33}\overline{V}_{35} + 2\overline{V}_{33}V_{35} + 2\overline{V}_{33}V_{55}\}.$$

Update $\hat{\omega}_4$ and $\hat{\theta}_3$ by solving $\hat{\lambda}(\mathrm{i}\omega) = -1 + \xi_1(\omega)\hat{\theta}^2 + \xi_2(\omega)\hat{\theta}^4 + \xi_3(\omega)\hat{\theta}^6 + \xi_4(\omega)\hat{\theta}^8$, and re-calculate $V_{33}, V_{35}, V_{37}, V_{55}, V_{57}$ and V_{77} at $\hat{\omega}_4$ to construct the periodic solution.

References

[1] Allwright DJ. Harmonic balance and the Hopf bifurcation theorem. Math Proc Cambridge Philos Soc 1977;82:453–67.
[2] Andersen CM, Geer JF. Power series expansions for the frequency and period of the limit cycle of the van der Pol equation. SIAM J Appl Math 1982;42:678–93.
[3] Atadan AS, Huseyin K. An intrinsic method of harmonic analysis for non-linear oscillations (a perturbation technique). J Sound Vib 1984;95:525–30.
[4] Basso M, Genesio R, Tesi A. A frequency method for predicting limit cycle bifurcations. Nonlinear Dynam 1997;13:339–60.
[5] Belhaq M, Freire E, Houssni M, Rodríguez-Luis AJ. Second period-doubling in a three-dimensional system. Mech Res Commun 1999;26:123–8.
[6] Berns DW, Moiola JL, Chen G. Detecting period-doubling bifurcation: an approximate monodromy matrix approach. Automatica 2001;37:1787–95.
[7] Buonomo A. On the periodic solution of the van der Pol's equation for small values of the damping parameter. Int J Circ Theor Appl 1998;26:39–52.
[8] Buonomo A, Di Bello C. Asymptotic formulas in nearly sinusoidal nonlinear oscillators. IEEE Trans Circuits Syst I 1996;43:953–63.
[9] Genesio R, Bagni G. A view of limit cycle bifurcations in relay feedback systems. IEEE Trans Circuits Syst I 2003;50:1134–40.
[10] Genesio R, Tesi A. Harmonic balance methods for the analysis of chaotic dynamics in nonlinear systems. Automatica 1992;28:531–48.
[11] Hale J. Oscillations in nonlinear systems. New York: Dover Pub. Inc.; 1963.
[12] Maggio GM, de Feo O, Kennedy MP. Nonlinear analysis of the Colpitts oscillator and applications to design. IEEE Trans Circuits Syst I 1999;46:1118–30.
[13] Mees AI. Dynamics of feedback systems. Chichester: John Wiley & Sons; 1981.
[14] Mees AI, Chua LO. The Hopf bifurcation theorem and its applications to nonlinear oscillations in circuits and systems. IEEE Trans Circuits Syst 1979;26:235–54.
[15] Mohan N, Undeland TM, Robbins WP. Power electronics, converters, application and design. Chichester: John Wiley & Sons; 1995.
[16] Moiola JL, Chen G. Hopf bifurcation analysis: a frequency domain approach. Singapore: World Scientific Publishing Co.; 1996.
[17] Qiu SS, Filanovsky IM. Periodic solutions of the van der Pol equation with moderate values of damping coefficient. IEEE Trans Circuits Syst 1987;34:913–8.

[18] Robbio FI, Alonso DM, Moiola JL. On semi-analytical procedure for detecting limit cycle bifurcations. Int J Bifurcat Chaos 2004;14(3):951–70.

[19] Strogatz SH. Nonlinear dynamics and chaos—with applications to Physics, Biology, Chemistry and Engineering. Cambridge: Perseus Books Publishing; 1994.